HEAT TRANSFER MEASUREMENTS OF A GASEOUS FUEL RIJKE COMBUSTOR UNDER OSCILLATORY AND NON-OSCILLATORY CONDITIONS

Cristiane Aparecida Martins
Instituto Tecnológico de Aeronáutica – São José dos Campos - SP
cmartins@ita.br

Marco Aurélio Ferreira
Instituto Nacional de Pesquisas Espaciais – Cachoeira Paulista - SP
marco@lcp.inpe.br

João Andrade de Carvalho Jr
Universidade Paulista - UNESP - Guaratinguetá
joão@feg.br

Abstract. *An experimental study has been conducted with the objective of investigating the effects of combustion driven acoustic oscillations in the transfer rate. The combustor operated with liquified petroleum gas (LPG) in both oscillatory and non oscillatory conditions, under the same input conditions. The main conclusion was: a) the pulsating combustion process is more efficient than the non pulsating process. This means that pulsating combustion must be more efficient to water heating.*

Keywords**: pulse combustion, transfer heat**

1. INTRODUCTION

Pulsating combustion can be considered an old matter. In fact, for more than a century, thermo-acoustic instabilities have been a concern for industries that involve combustion processes. These instabilities were first observed in 1777 by Higgins who observed the so called hydrogen ‘singing’ flames in tubes. After that, several experiments were initiated, among them, the one by Rijke, in 1859. Rijke discovered that strong acoustic oscillations occurred when a heated metallic grid was positioned in the lower half of a vertical tube opened at both ends (Lord Rayleigh, 1945). This were subsequently documented by Tyndall (Tyndall, 1970) in 1897 and scientifically explained in 1878 by Lord Rayleigh with his famous criterion that describes the mechanism by which heat release could excite acoustic waves [Zinn, 1986]. Rayleigh concluded that pressure amplification will occur if heat release fluctuations are in phase with the resultant pressure fluctuations.

Since them, researchers have used Rayleigh’s criterion to determine the tendency of any combustion process to go unstable due to thermo-acoustic instabilities. Although all of these researchers have been directed towards understanding, predicting and controlling thermo-acoustic instabilities, there is no consensus on the most definitive solution to the problem yet. Still the most widely investigated system, to study these thermo-acoustic instabilities is the Rijke tube, probably due to its simplicity and ease for conducting experiments under controlled laboratory conditions. Figure 1 shows a schematic of the Rijke tube. Rijke tube is simply a cylindrical tube with both ends open, and a heat source placed inside of it. The heat source may be a flame or an electrical heating element. Whenever the energy source is placed in the lower half of the Rijke tube, it results in self-excited acoustic oscillations while placing the energy source in its upper half attenuates any acoustic oscillations. Raun et al. (1993) presents a detailed literature review of the work on the Rijke tubes, and discusses the physical mechanisms that are responsible for the thermo-acoustic oscillations for various energy sources such as, wall temperature gradients, electrically heated wire gauze and combustion.

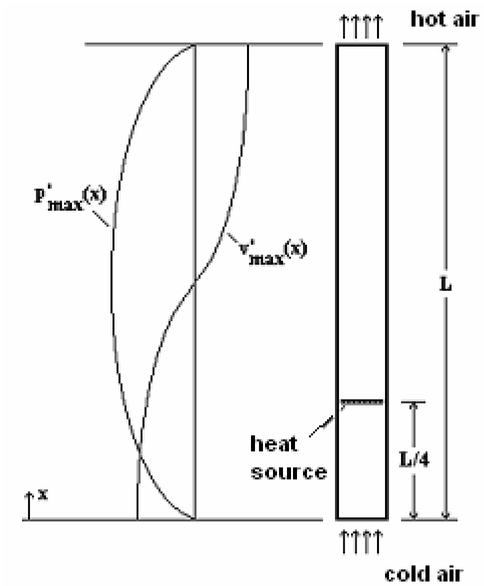

Figure 1: Schematic of a Rijke tube depicting the first mode instability.
(a) Pressure and velocity mode shape.

The present study investigates the effects of combustion driven acoustic oscillations in the heat transfer rate of a Rijke-type pulse combustor. The fuel utilised in the experiments was liquefied petroleum gas (LPG) and the combustor operated, both in oscillatory and non-oscillatory regimes, under the same input conditions. Firstly, the experimental installation will be described.

2. EXPERIMENTAL DESCRIPTION

Rijke tube, shown in Fig. 2, consists of a cylindrical tube made of steel open at both ends. It is a water-jacketed 2.80-m long by 7.2-cm internal diameter stainless steel vertical tube. The length of the diameter ratio is around 39 – this is more than sufficient to consider the acoustic waves one-dimensional in nature. Inside the Rijke tube there is one gauze metal which played the part of the flame holder. At the bottom there is one decoupling chamber with 60-cm long by 39.5-cm internal diameter. This chamber is needed to provide control of the combustion air flow rate without disturbing the required open-end boundary condition at the tube entrance. A radial compressor, IBRAM model CR-8, provided combustion air. Fuel was provided by some commercial 45 kg LPG cylinders. The fuel gas (LPG) used is a mixture of hydrocarbons. Its formula can be taken as $C_{3.425}H_{7.824}$, with a molecular weight of 49 g/gmol. Its theoretical fuel/air ratio is 3.89E-2 (molar basis). Both LPG and air flow rates were measured with orifice plate flowmeters.

Temperatures and acoustic pressures were measured with six chromel/alumel thermocouples and four piezoelectric pressure transducers, Kistler (model 7261). The positions of both of them were shown in Fig 2. The transducers were individually connected to charge amplifiers (model 5006). Both thermocouple and pressure transducer signals were stored and analysed by a computerised data system.

The L shape sample probe was installed in one region where the gas composition is already in steady state. The sampled gas followed from the combustor output to the cooling and cleaning systems. After that, the flue gas was led towards continuous gas analysers: infrared for CO, thermomagnetic for O_2, and chemiluminescent for NO_x (Fisher-Rosemount model 951) Data were collected for each test setting during 15 min, after a minimum of 5 min period, for which O_2 concentration stabilised. Each data point is a result of an average of at least 30 collected data. Each experimental condition was repeated at least three times in different days. The idea is to obtain reproducibility.

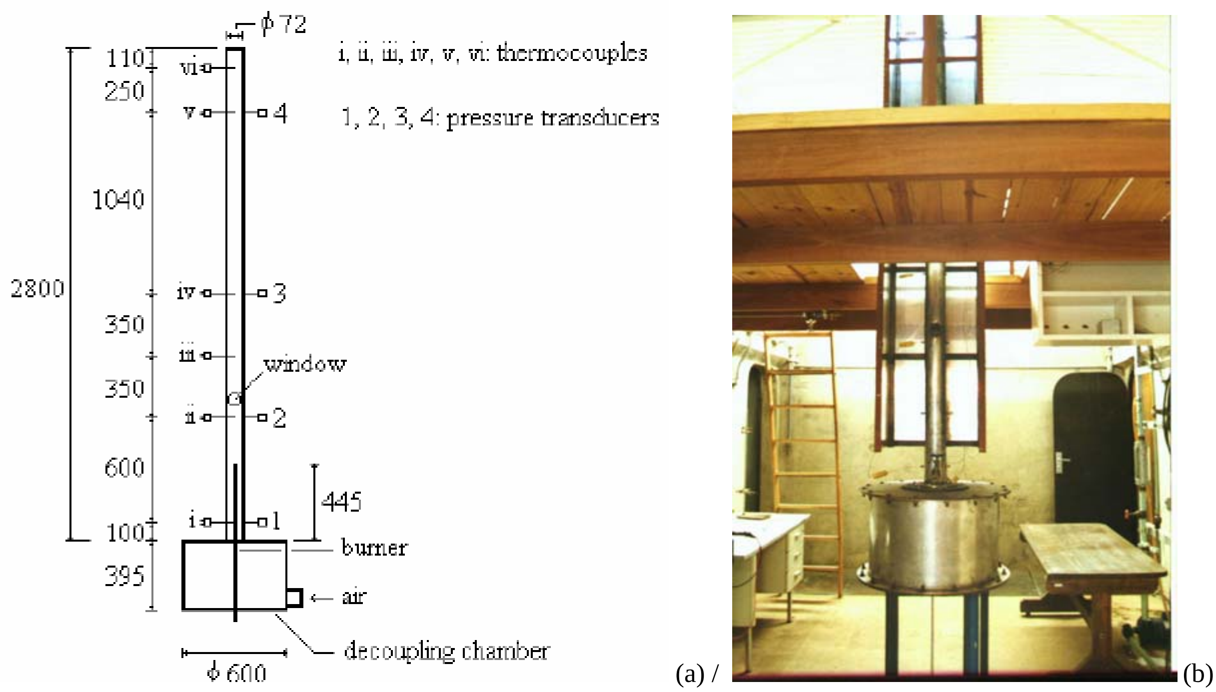

Figure 2: Rijke tube. (a) Dimensions in mm. (b) Rijke installation

The burner, shown in Fig. 3 has a main body which possesses a nominal diameter of 1.2 cm. Its length was nearly 3 cm, which could be increased by the addition of segments. The fuel was discharged through six 1-mm diameter holes. By inserting A in the burner, pulse combustion was achieved. Without this part, the flow of gas became exclusively longitudinal and acoustic oscillations were not even generated with this burner configuration. In this way it was possible to keep the same residence time above the burner location for pulsating and non-pulsating combustion.

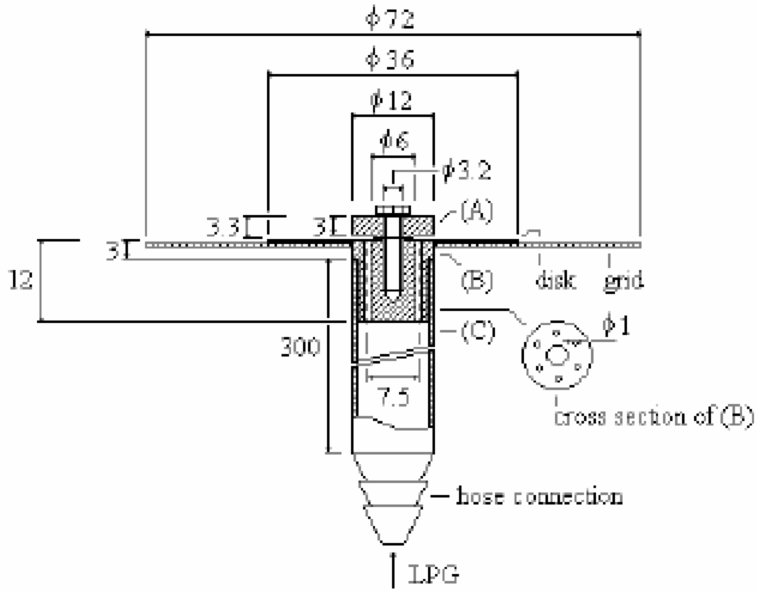

Figure 3 - Burner details

The burner was placed at 45 cm from the base of the combustor. This position, for tests with insert A, kept the flame concentrated in the lower half of the tube and, in this way, Rayleigh criterion was satisfied for the first mode of oscillation. No change in turbulence was resulted by the attachment of insert A, since no adjustment in the flow control valve was required to keep the fuel gas flow rate constant in both situations, pulsating and non-pulsating.

Temperature, pressure dynamics and gases concentrations signals were sent to data acquisition. At the heart of any data acquisition system lays the data acquisition hardware. The main function of this hardware is to convert analog signals to digital signals, and to convert digital signals to analog signals. For example, the basic setup used during the acquisition of thermocouple data, involved attaching thermocouple probes to a low voltage analog/digital data acquisition board of National Instruments. The board was connected to a high resolution National Instruments data acquisition card (PCI 6025-E) with a built-in analog-to-digital converter. The signal was acquired, saved, and analyzed using National Instruments LabView® software. The setup had the capability of visualizing the signal in real time and performing all the post- processing at the same time the signal was being acquired. The data collection system was equipped with an internal reference to avoid the need to set up and maintain an ice bath reference junction. The computer provides a processor, a system clock, a bus to transfer data, and memory and disk space to store data. Data acquisition software allows exchanging information between the computer and the hardware. Typically, the software allows the configuration of the sampling rate of your board, and acquires a predefined amount of data. The Data acquisition system used is showed in Figure 4.

Figure 4- Data acquisition system

3. PULSATING AND NON-PULSATING EXPERIMENTAL CONDITIONS

The LPG flow rates chosen for the tests were 0.15 and 0.30 g/s, corresponding to total residence times on the order of 1 and 2 s, respectively (residence times varied with air excess). Considering PCI of the fuel equal 45217.44 kJ/kg, it produces the potency of the 6.9 and 13.8 kW respectively. Constant flow cooling water of the 15 litters/min through the jacket was fixed for all experiments. Also measurements were got without a water jacket flow. They are put in the first paragraph in the next section.

The flow rate of the air utilised in the tests varied from 2.0 to 3.5 g/s at 0.15 g/s fuel rate and from 4.0 to 7.0 g/s at 0.30 g/s fuel rate

The equivalence ratio is defined as $\left(\dfrac{\dot{m}_F}{\dot{m}_{AIR}}\right) \Big/ \left(\dfrac{\dot{m}_F}{\dot{m}_{AIR}}\right)_{STOIC}$ where $\dot{m}_{AIR}$ is the air flow rate, $\dot{m}_F$ if the fuel feed rate and $\left(\dfrac{\dot{m}_F}{\dot{m}_{AIR}}\right)_{STOIC}$ is fuel feed rate and air flow rate a stoichiometric relation.

Firstly, the O_2 concentration was plotted as a function of the calculated equivalence ratio for both regimes, pulsating and non pulsating, Fig. 4. It can be observed that values of O_2 concentration practically fell on the same line for both regimes; therefore, possible errors were discarded in the mean mass flow rates for the pulsating case.

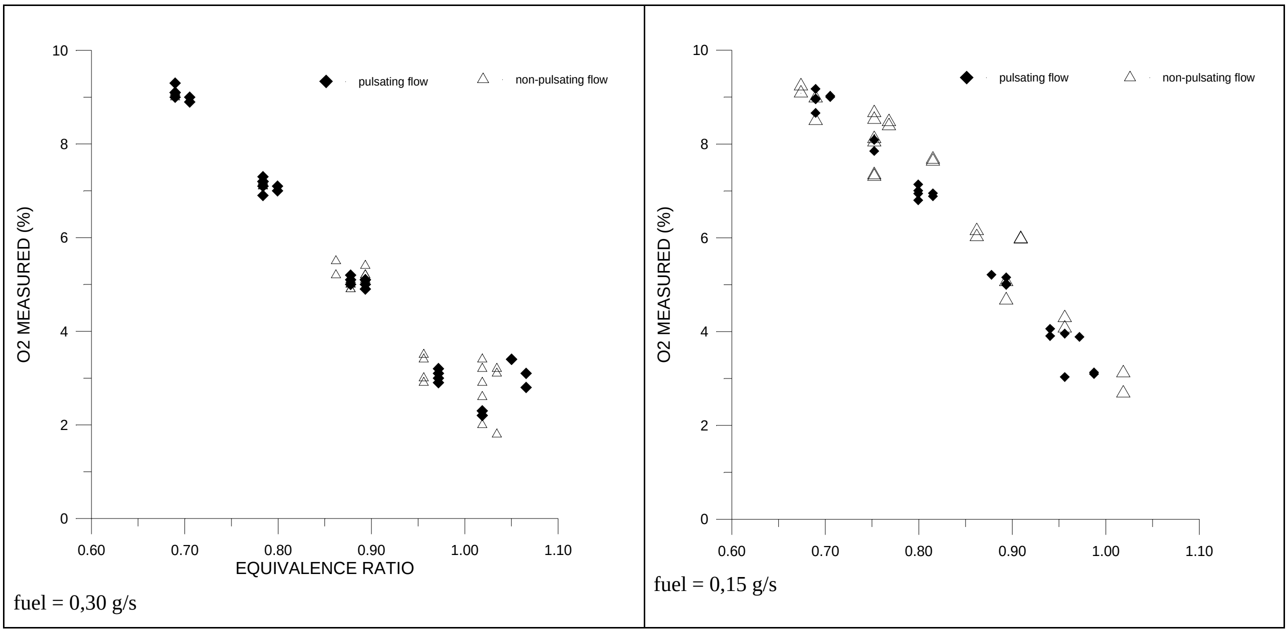

Figure 4 - Oxygen measurements versus equivalence ratio in both regimes - pulsating and non-pulsating flow.

4. RESULTS AND DISCUSSION

Experiments were conducted to quantify the total heat transfer process from the flame and burned gases to Rijke combustor internal wall. Frequency is lower for the lower LPG mass flow rate (72 to 76 Hz for 0.15 g/s, and 78 to 83 Hz for 0.30 g/s. The frequency depends on the square root of average absolute temperature, which is higher for the higher input rate of fuel.

4.1 Pressure amplitude effects

Firstly, as previously mentioned, the results obtained will be showed with any cooling fluid through the jacket under pulsating regime. In Figure 5 (a)to(i) it is plotted the magnitude of amplitude of pressure (Pa) as abscissa and Exhaust heat loss (% LHV) as ordinate and also described the equivalence ratio in each case. Increase in pressure amplitude means higher heat transfer through the tube. This is the same as the lower exhaust heat loss (%). One critical exception is observed in Figure 5 (f) to condition of the 6840 Pa.

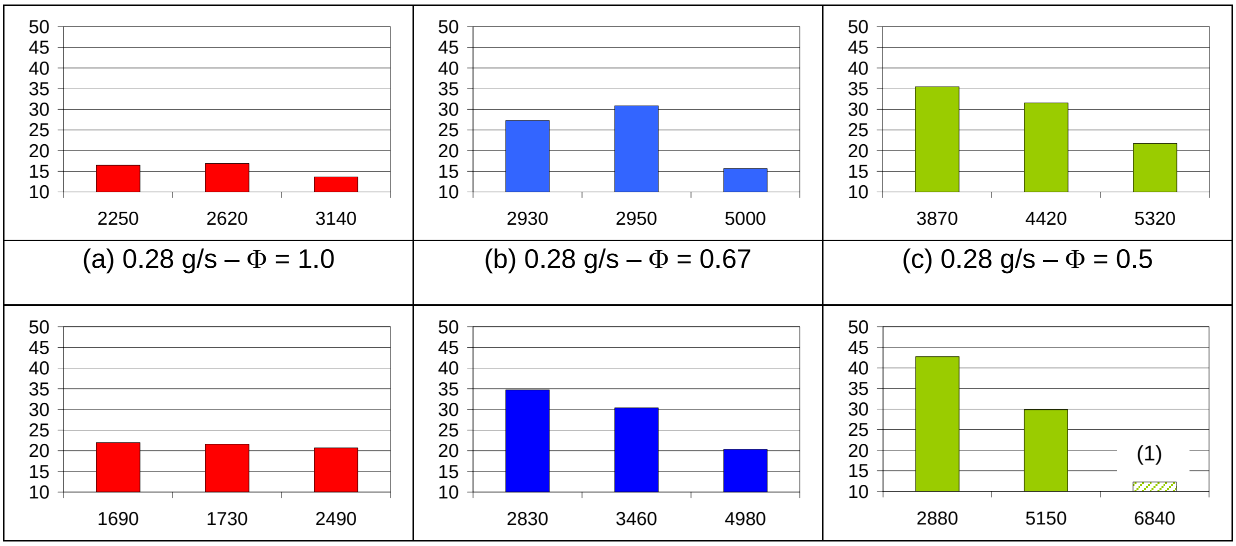

(d) 0.35 g/s – Φ = 1.0	(e) 0.35 g/s – Φ = 0.67	(f) 0.35 g/s – Φ = 0.5
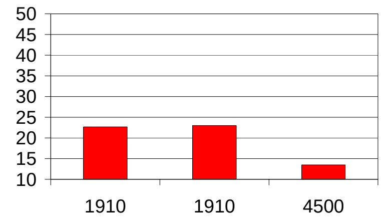	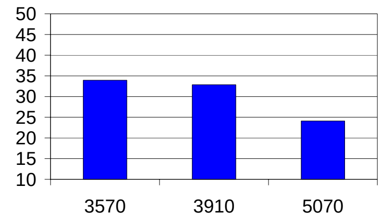	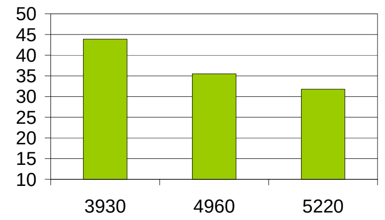
(g) 0.39 g/s – Φ = 1.0	(h) 0.39 g/s – Φ = 0.67	(i) 0.39 g/s – Φ = 0.5

Figure 5 . Exhaust heat loss (% LHV) x acoustic pressure amplitude (Pa) in a Rijke combustor 2.8 m long and 74.5 mm internal diameter, without water jacket, 81 < f < 85 Hz

Figure 5(f) with 6840Pa condition can be explained due to a stream reversal development at the end of the pipe, due to periodical alterations of the flow direction. Considering some solutions of the wave equation to ends open tube, isotherm condition is given by:

$$p' = c\bar{\rho}\left(A\,\mathrm{sen}\frac{\omega x}{c} - B\cos\frac{\omega x}{c} \right)\mathrm{sen}\,\omega t$$

and

$$u' = \left(A\cos\frac{\omega x}{c} + B\,\mathrm{sen}\frac{\omega x}{c} \right)\cos\omega t\,.$$

Starting with one of the open extremities as coordinates of the initial condition in one 1/2 wave tube, the boundary conditions to acoustic pressure are $p'(0,t) = 0$ e $p'(L,t) = 0$. This means that:

$$p' = c\bar{\rho}A\,sen\frac{\omega x}{c}\,sen\,\omega t = c\bar{\rho}A\,sen\frac{n\pi x}{L}\,sen\frac{n\pi c t}{L}\,,$$

and

$$u' = A\cos\frac{\omega x}{c}\cos\omega t = A\cos\frac{n\pi x}{L}\cos\frac{n\pi c t}{L}$$

But, $\omega = 2\pi\, f_n$ is the angular frequency, then the frequencies of the oscillations mode are given by: $f_n = \dfrac{nc}{2L}$.

Magnitude of pressure amplitude (Pa) can be experimentally obtained with a pressure transducer (as in this work) or with a microphone. It enables the evaluation of the constant A in early equations:

$$p'_{máx} = Ac\bar{\rho} \text{ e } u'_{máx} = A = \frac{p'_{máx}}{c\,\bar{\rho}}\,.$$

The displacement x' is obtained through the integration the u' in time:

$$x' = \frac{A}{\omega}\cos\frac{\omega x}{c}\,sen\omega t\,,$$

where:

$$x'_{máx} = \frac{A}{\omega} = \frac{A}{2\pi\, f_n} = \frac{AL}{n\pi c}\,.$$

Considering the displacement promoted by the mean velocity: $x = \bar{u}\,t + x'$,

or:

$$x = \bar{u}\,t + \frac{p'_{máx}\,L}{n\pi\,\bar{\rho}\,c^2}\cos\frac{n\pi x}{L}\,sen\frac{n\pi c t}{L}\,.$$

For example, 80 Hz and mean temperature equal 773 K, with the pressure amplitude equal 7000 Pa the acoustic displacement in tube end can be reached to 55 mm. This consideration allowed the external air to be admitted as a reversal flow in the end of the pipe. Otherwise to pressure amplitude equal 2000 Pa means displacement approximately of the 16 mm.

4.2 Pulsating versus Non-Pulsating

Figure 6 presents Exhaust heat loss (% LHV) x equivalence ratio in a Rijke combustor 2.8 m long and 72 mm internal diameter, with water jacket, , 66 < f < 83 Hz. It can be observed that the presence of pulsations increase the rate of heat transfer from the combustion products to the walls of the pipe. This can allow one reduction in the size and cost of the system. The back-and forth oscillations of the gases inside the tube, produced by the acoustic fields, increase the efficiency of mixing between the air and fuel, which is able to reduce the amount of air required to complete the burn. It can be observed that for the same exhaust loss pulsating regime, it is able to burn more fuel (0.23 g/s versus 0.13 g/s) in relation non-pulsating flow.

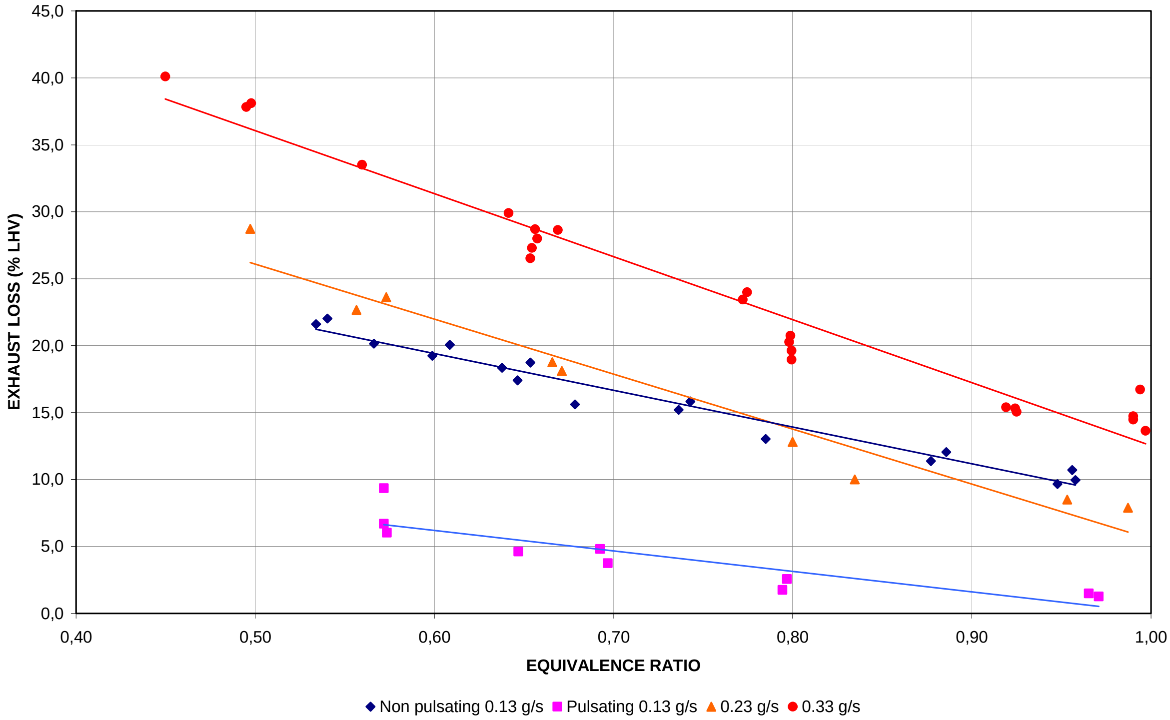

Figure 6: Exhaust heat loss (% LHV) x equivalence ratio in a Rijke combustor 2.8 m long and 72 mm internal diameter, with water jacket, , 66 < f < 83 Hz.

Another way to visualize the phenomenon is by separating the heat transfer into three parts. All the following results assume that the axial conduction in the thin pipe wall is negligible. The flow cooling water remains constant during the whole experiment in the pulsating or non-pulsating regimes, always 15 litters /min through the jacket. The heat transferred to the wall is calculated considering experimental measurements of the temperature outlet minus the temperature inlet and the mass flow of the water flow, this is here called as Q cooling jacket. The following equations were utilised to obtain energy distribution.

Exhaust flow (kg/s) = air flow (kg/s) + fuel flow (kg/s)

Q fuel (kW) = fuel flow (g/s) * PCI (45,21744MJ/kg)

Q cooling jacket (kW) = cooling flow (kg/s) * Cp cooling (4,1813 kJ/kgK) * Tout (°C) – Tin (°C)

Q exhaust (kW) = Exhaust flow (kg/s) * Cp exhaust (mean value) (1.1kJ/kgK) * Tout (°C) – Tin (measured)

Q environment (calculated) = Q fuel – (Q cooling jacket – Q exhaust)

Figures 7-8 (a) and (b) respectively presents the effect of different operating conditions in each part of the total heat transfer, the temperature measurements are on the right side. The mass flux rate is 0.15 g/s and the air flow was increased from 2.4 to 3.4 g/s. It is possible to observe that the pulsating flow in all range fuel-air ratio could be increased at the heat transfer. Temperature profile is well defined in pulsating regime, the opposite is observed in non-pulsating flow.

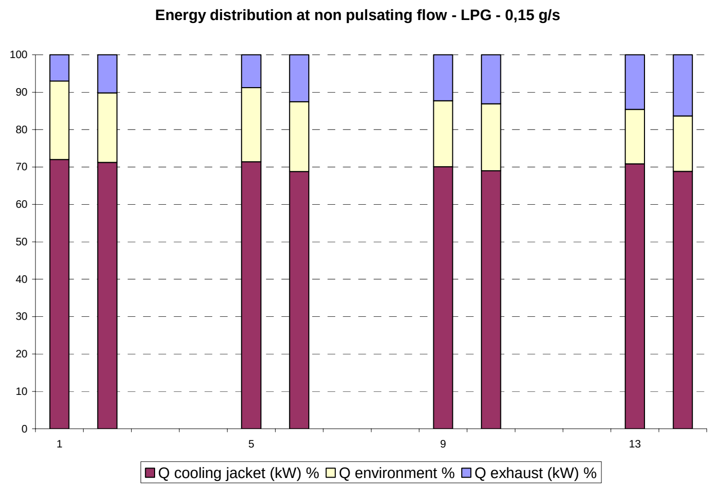

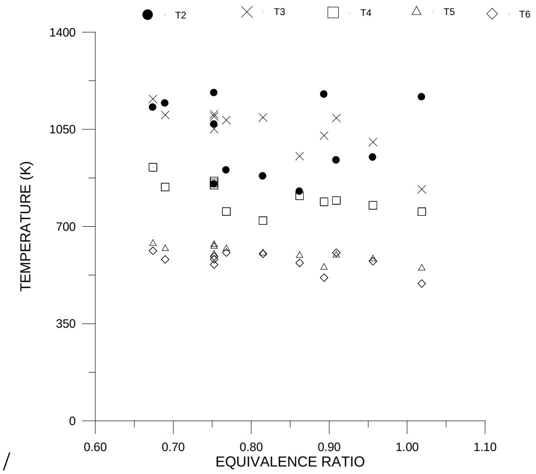

(a) (b)

Figure 7 - (a) Energy distribution to 0,15 g/s non pulsating flow -
Sequences: 1, 5, 9, 13 corresponding to 1.0, 0.9, 0.8 and 0.7 Equivalence Ratio values.
(b) Temperature measured to 0, 15g/s non pulsating flow

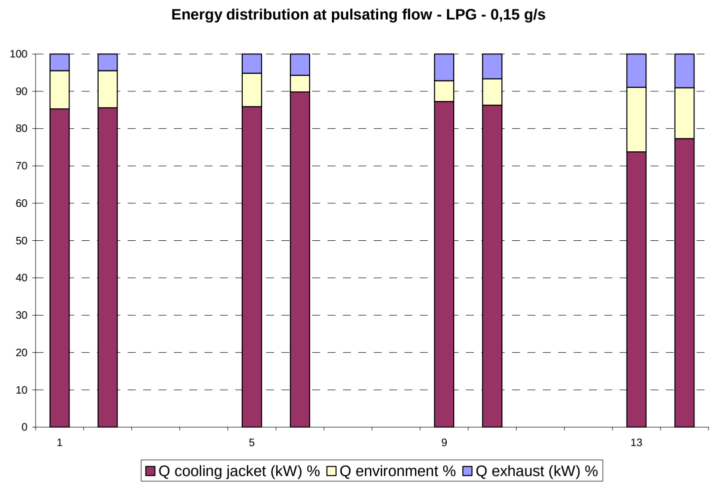

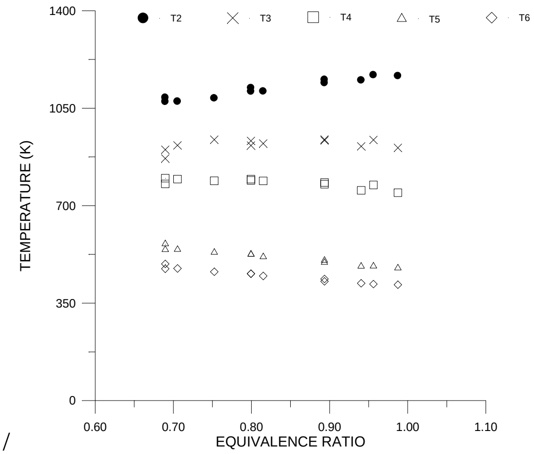

(a) (b)

Figure 8 - Energy distribution to 0,15 g/s pulsating flow -
Sequences: 1, 5, 9, 13 corresponding to 1.0, 0.9, 0.8 and 0.7 Equivalence Ratio values.
(b) Temperature measured to 0, 15g/s pulsating flow

The changes in the local flame properties associated with this range of fuel-air ratio and pulsating seem not to be significant to alter the general trend of the total heat flux distributions. In Fig. 9-10 (a) and (b) constant fuel flow rate equals 0,3 g/s, the results indicated that the increase in the fuel-air ratio has a small effect on the observed total heat flux values.

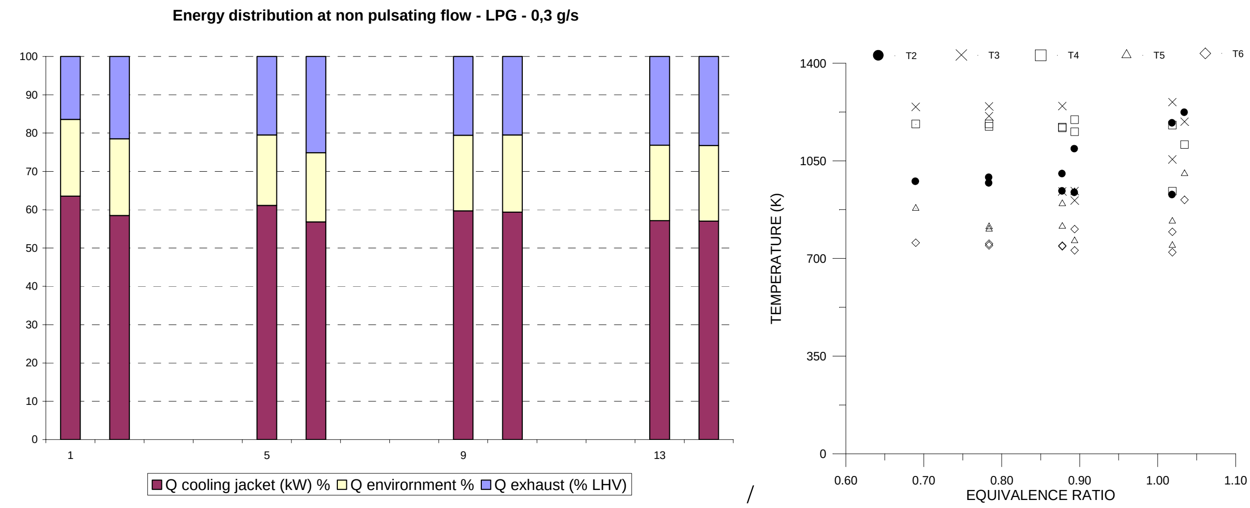

(a) (b)

Figure 9 - (a) Energy distribution to 0,3 g/s non pulsating flow -
Sequences: 1, 5, 9, 13 corresponding to 1.0, 0.9, 0.8 and 0.7 Equivalence Ratio values
(b) Temperature measured to 0, 30g/s non pulsating flow

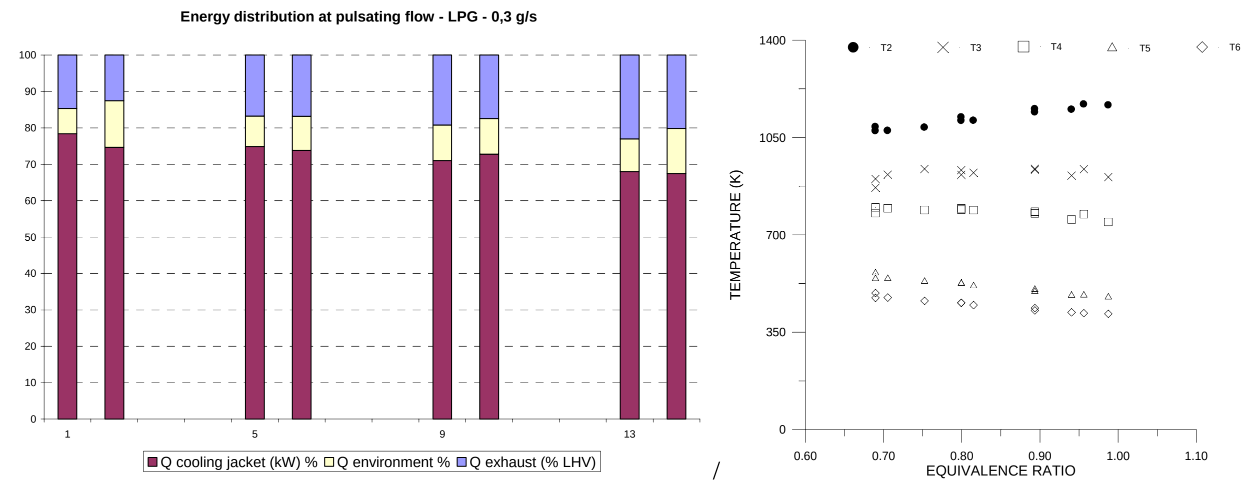

(a) (b)

Figure 10 - (a) Energy distribution to 0,30 g/s pulsating flow -
Sequences: 1, 5, 9, 13 corresponding to 1.0, 0.9, 0.8 and 0.7 Equivalence Ratio values.
(b) Temperature measured to 0, 30g/s pulsating flow

5. CONCLUSION

This work aims to present the experimental results, but a deeper discussion is still necessary. Pulsating combustion still remains as a challenge. Pulsating phenomena have the experimental investigation as one of the most reliable way to understand the phenomenon. It is known that independent on the system under consideration, the criterion to maintain the heat driven oscillations in any system requires the pressure field and heat release to be in phase (Rayleigh, 1878). But, until now, at least to Rijke combustor, it is not possible to obtain an amplitude pressure control. This means that the reactant supply processes, chemical kinetics and fluid mixing need to be synchronized with the pressure field so that the heat is released around or at the peak pressure to reinforce the resonant condition and to overcome all system losses. There have been numerous valuable studies undertaken identifying the different phenomena required to phase match the heat release and the resonant pressure field, such as the role of coherent structures, characteristic time, ignition delay, and periodic flame stretch.

6. REFERENCES

Lord Rayleigh, *The Theory of Sound*. Dover, New York, 1945.

Tyndall, J., *J. Physical Sciences* 2:30-37, 1970.

Raun R. L. , Beckstead M. W., Finlinson J. C. and Brooks, K. P., A review of Rijke tubes, Rijke burners and related devices, Progress in Energy and Combustion Science, Volume 19, Issue 4, 1993, Pages 313-364

Zinn, B.T., Pulsating Combustion, in *Advanced Combustion Methods* (ed. F.J. Weinberg), Academic Press, 113-181, 1986.

7. RESPONSIBILITY NOTICE

The author(s) is (are) the only responsible for the printed material included in this paper.